7
-15-91 JS (2)

LBL-30668
UC-~~400~~ 414

Lawrence Berkeley Laboratory
UNIVERSITY OF CALIFORNIA

Accelerator & Fusion Research Division

Magnetic Field in the SSC Arc Quad.

S. Caspi, M. Helm, and L.J. Laslett

April 1991

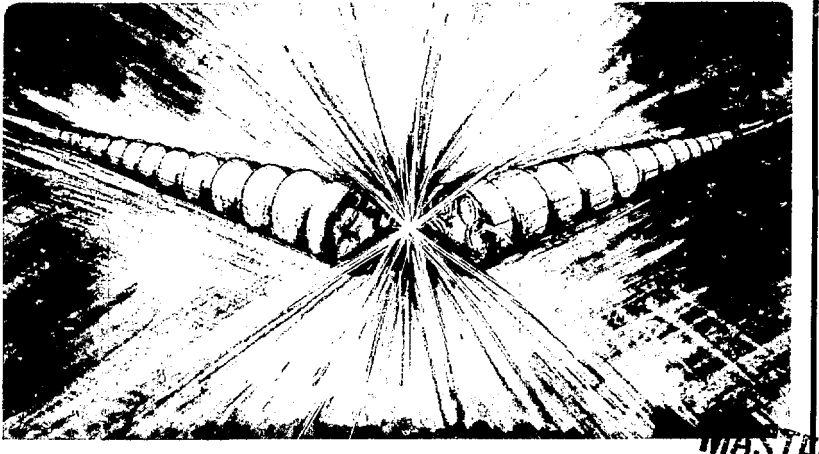

MASTER

Prepared for the U.S. Department of Energy under Contract Number DE-AC03-76SF00098

DISTRIBUTION OF THIS DOCUMENT IS UNLIMITED

DISCLAIMER

This document was prepared as an account of work sponsored by the United States Government. Neither the United States Government nor any agency thereof, nor The Regents of the University of California, nor any of their employees, makes any warranty, express or implied, or assumes any legal liability or responsibility for the accuracy, completeness, or usefulness of any information, apparatus, product, or process disclosed, or represents that its use would not infringe privately owned rights. Reference herein to any specific commercial product, process, or service by its trade name, trademark, manufacturer, or otherwise, does not necessarily constitute or imply its endorsement, recommendation, or favoring by the United States Government or any agency thereof, or The Regents of the University of California. The views and opinions of authors expressed herein do not necessarily state or reflect those of the United States Government or any agency thereof or The Regents of the University of California and shall not be used for advertising or product endorsement purposes.

Lawrence Berkeley Laboratory is an equal opportunity employer.

LBL--30668

DE92 000656

Magnetic Field In the SSC Arc Quad.*

S.Caspi, M.Helm and L.J. Laslett

Lawrence Berkeley Laboratory
University Of California
Berkeley, CA 94720

April 29, 1991

* This was supported by the Director, Office of Energy Research, Office of High Energy and Nuclear Physics, High Energy Physics Division, U. S. Department of Energy, under Contract No. DE-AC03-76SF00098.

MASTER

DISTRIBUTION OF THIS DOCUMENT IS UNLIMITED

Abstract

In part one we report on field calculations along the conductor in the end region of the SSC arc-quad. We have determined that the maximum field in the 2D section is 5.04 tesla located at the pole turn of the inner layer somewhere in the middle of the cable (strand 9)(fields are at 6500 A[†]. At the "end" the maximum field is slightly higher 5.09 tesla located at the overpass (strand 11). The iron contribution was included assuming infinite permeability. In part two we include results of a 3D representation of the magnetic field inside the bore. The complete analysis, for which a brief description has been included here , is described elsewhere[‡]. This form for presenting the field is suitable for interfacing with other codes that make use of the 3D field components (particle tracking and stability).

Part 1 — maximum field at the conductor

The conductor geometry and fields are summarized in the following figures.

---

† The 40 mm SSC Arc Quadrupole – Magnetic Design — S.Caspi , M.Helm , and L.J. Laslett , SC-MAG-314 , LBID—1677 , November 1990.

‡ 3D Field Harmonics — S.Caspi , M.Helm , and L.J. Laslett , SC-MAG-328 , LBL-30313 , March 1991.

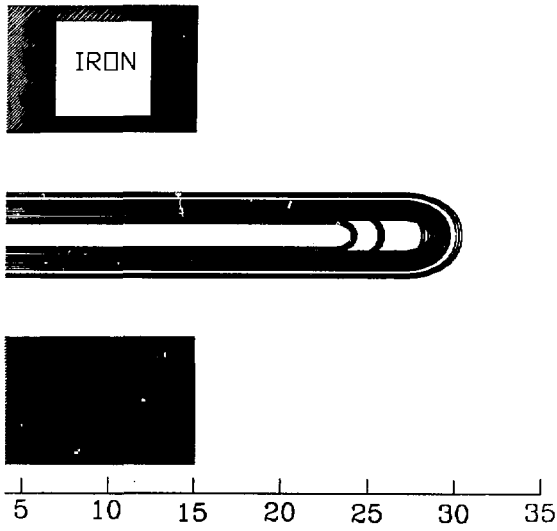

Figure 1 Coil schematic and IRON location in the end region.

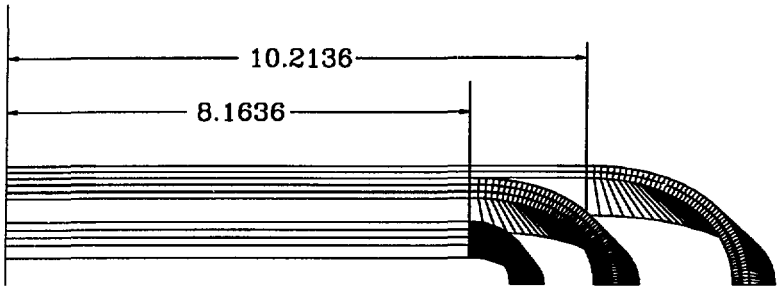

Figure 2 Conductor geometry in the end region of the SSC quad — LAYER-1 TOP.

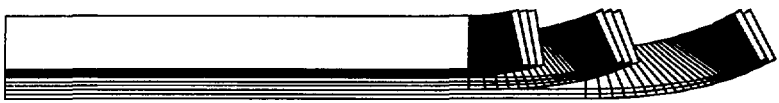

Figure 3 Conductor geometry in the end region of the SSC quad — LAYER-1 SIDE.

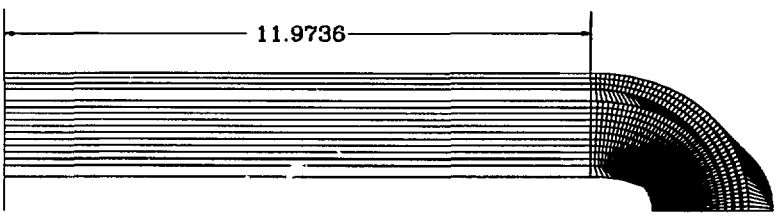

Figure 4 Conductor geometry in the end region of the SSC quad — LAYER-2 TOP.

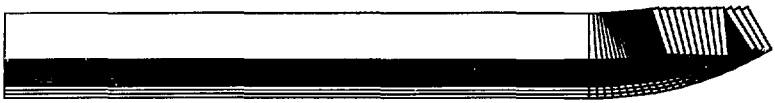

Figure 5 Conductor geometry in the end region of the SSC quad — LAYER-2 SIDE.

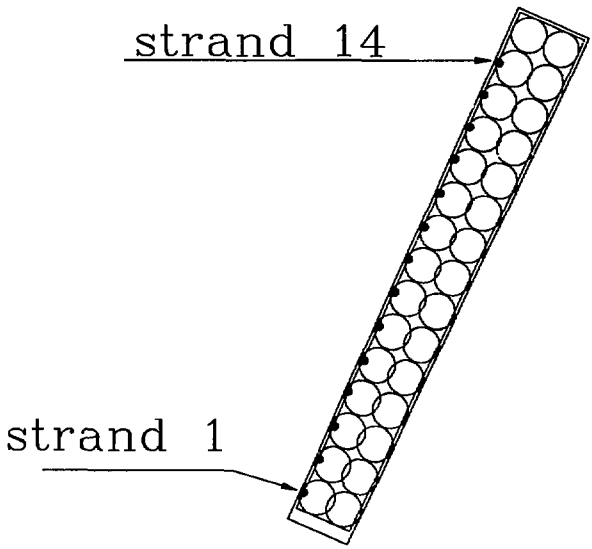

Figure 6 Strand number and location where fields have been calculated.

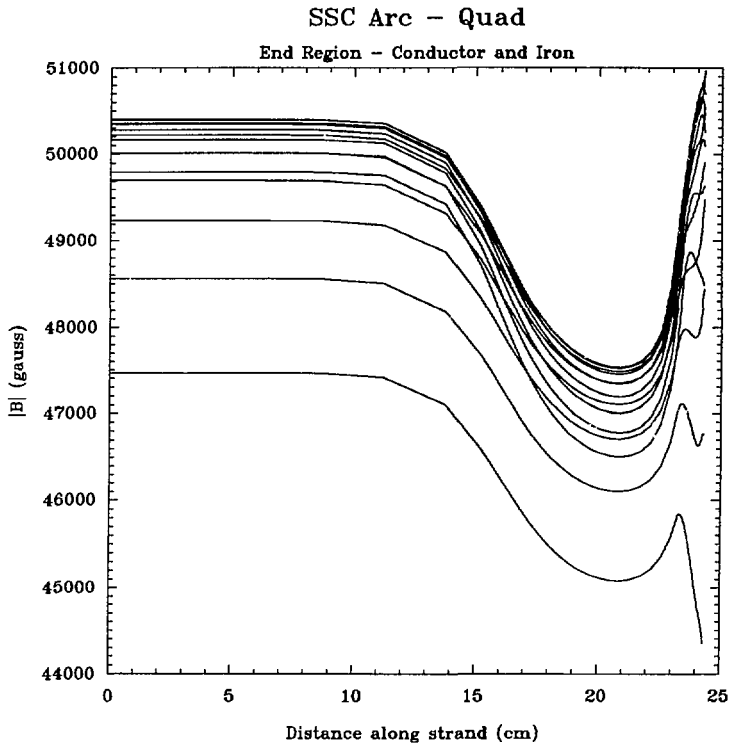

Figure 7 Absolute field along pole turn.

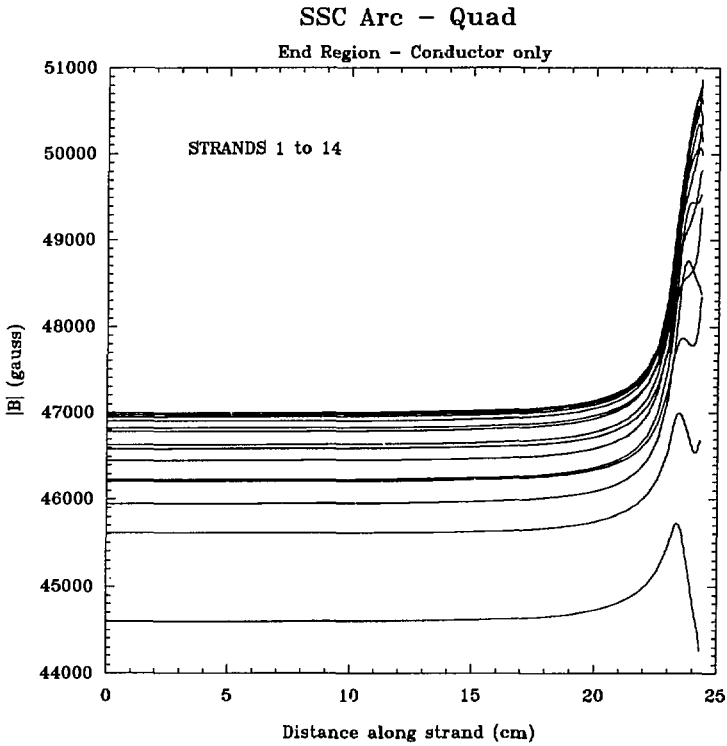

Figure 8 Absolute field along pole turn — CONDUCTOR ONLY.

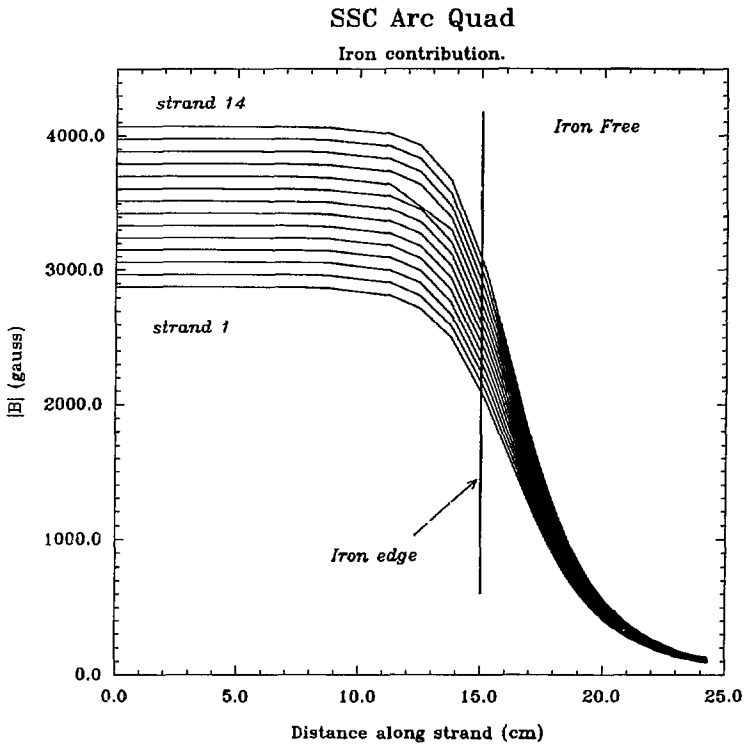

Figure 9 Absolute field along pole turn — IRON ONLY.

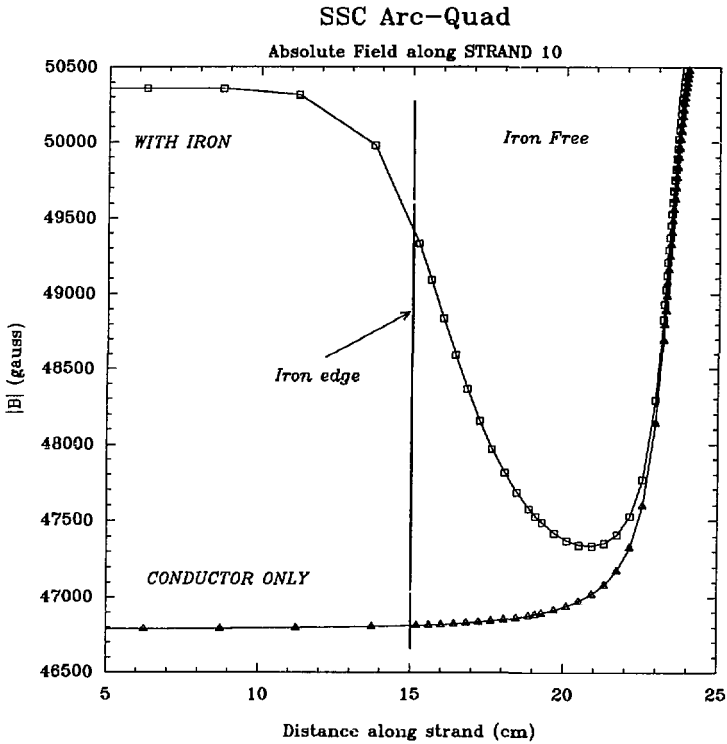

Figure 10 Absolute field along strand 10 — with and without iron.

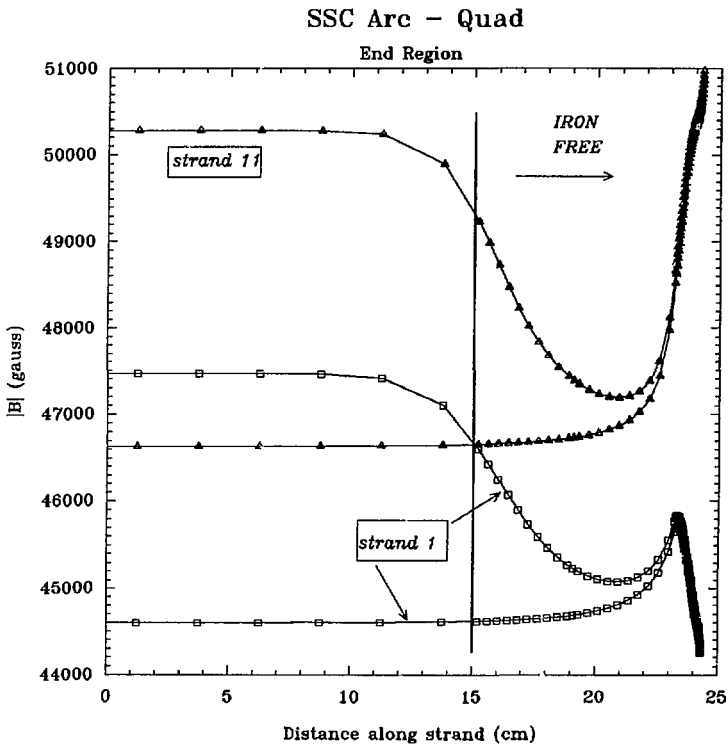

Figure 11 Absolute field along strands 1 and 11 — with and without iron.

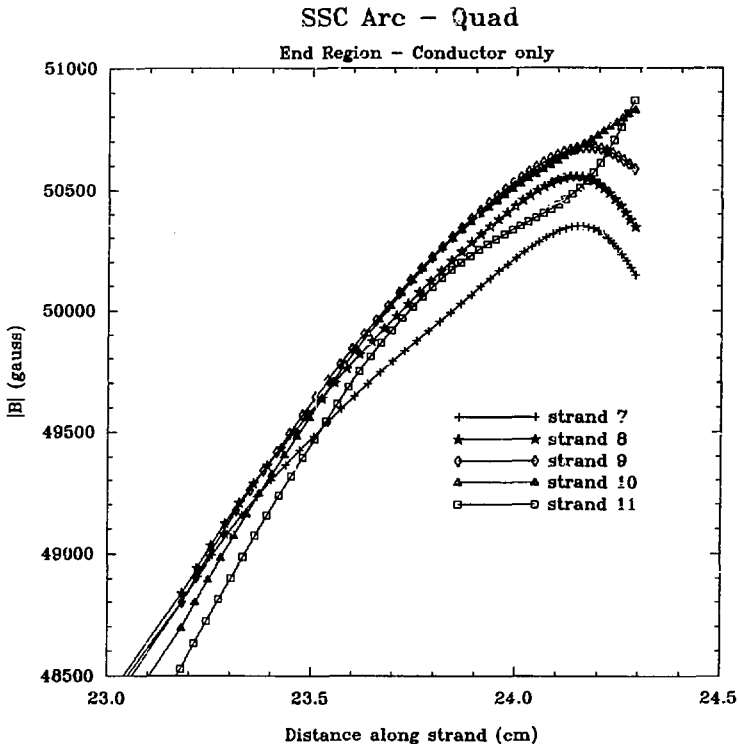

Figure 12 Absolute field at the end overpass.

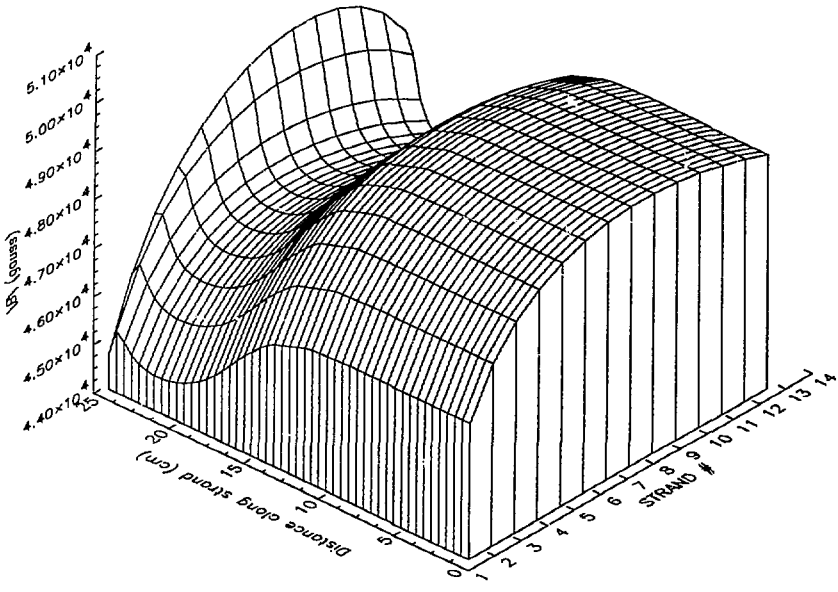

Figure 13 A 3 dimensional plot of the field magnitude as a function of strand number and position along the cable — view is from the straight section towards the "end".

Forces and Torque

We demonstrate a possible detailed calculation by producing the field around the strands of the pole turn of the inner layer in the straight section. The figure below shows the locations where the fields have been calculated. The next figure plots the absolute field at each location. The force on this turn was calculated to be Fx=131 lb/inch , Fy=-107 lb/inch.

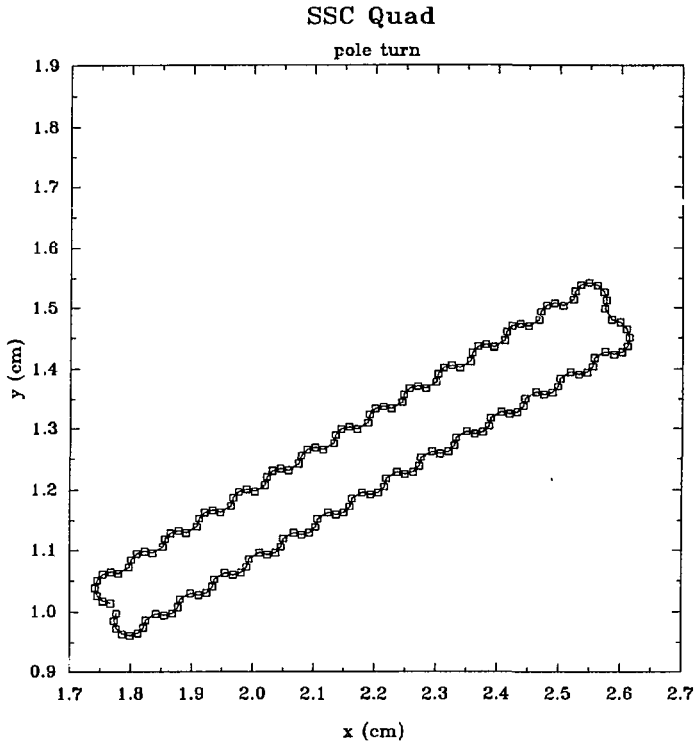

Figure 14 XY location around pole turn where field is calculated.

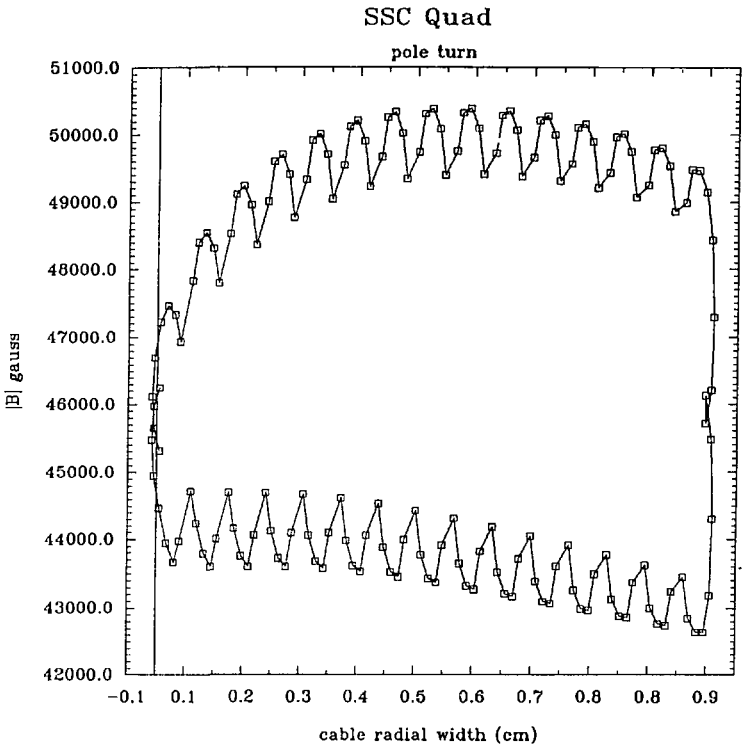

Figure 15 Absolute fields around cable.

Part 2 — 3D Field Components inside the bore.

We note that in the curl-free divergence-free region near the axis r=0 the field components may be expressed as given by $\vec{B} = -\nabla V$ where V is a scalar potential function for which $\nabla^2 V = 0$. The proposed solution can be written in the form :

$$V = \sum_{n=1} V_n(r,z) \sin n\theta$$

$$with: \tag{1}$$

$$\frac{1}{r}\frac{\partial}{\partial r}\left(r\frac{\partial V_n}{\partial r}\right) + \frac{\partial^2 V_n}{\partial z^2} - \frac{n^2 V_n}{r^2} = 0$$

We note that if V_n were to be free of any z-dependence, the acceptable solution for V_n near the axis would be expressed by a single term proportional to r^n (i.e., involving r raised to the positive power n); more generally one would represent V_n by a power series involving factors r^{n+2k}, commencing with r^n, and employing z-dependent coefficients :

$$V_n = \sum_{k=0} C_{n,k}(z) r^{n+2k}$$

$$with\ C_{n,k}(z)\ satisfying\ the\ recursion\ relation \tag{2}$$

$$C_{n,k}(z) = -\frac{1}{4k(n+k)}\frac{d^2 C_{n,k-1}}{dz^2} \quad ; \quad k = 1, \ldots$$

The magnetic field can be derived accordingly as :

$$\begin{aligned} B_{r,n} &= -\frac{\partial V_n}{\partial r}\sin n\theta = g_{rn} r^{n-1}\sin n\theta \\ B_{\theta,n} &= -\frac{n}{r}V_n \cos n\theta = g_{\theta n} r^{n-1}\cos n\theta \\ B_{z,n} &= -\frac{\partial V_n}{\partial z}\sin n\theta = g_{zn} r^n \sin n\theta \end{aligned} \tag{3}$$

In order that the series for V_n satisfy the differential equation written above we introduce $A_n(z)$ and express the coefficients g_{rn} , $g_{\theta n}$ as general functions of r and z as shown below :

$$\begin{aligned} g_{rn}(r,z) &= \sum_{k=0}(-1)^{k+1}\frac{n!(n+2k)}{2^{2k}k!(n+k)!}A_n^{(2k)}(z) r^{2k} \\ g_{\theta n}(r,z) &= \sum_{k=0}(-1)^{k+1}\frac{n!n}{2^{2k}k!(n+k)!}A_n^{(2k)}(z) r^{2k} \end{aligned} \tag{4}$$

Explicitly we can write the above as :

$$\begin{aligned} g_{rn}(r,z) &= -nA_n(z) + \frac{n+2}{4(n+1)}A_n''(z)r^2 - \frac{n+4}{32(n+1)(n+2)}A_n''''(z)r^4 \\ &\quad + \frac{n+6}{384(n+1)(n+2)(n+3)}A_n'''''''(z)r^6 - \ldots \\ g_{\theta n}(r,z) &= -nA_n(z) + \frac{n}{4(n+1)}A_n''(z)r^2 - \frac{n}{32(n+1)(n+2)}A_n''''(z)r^4 \\ &\quad + \frac{n}{384(n+1)(n+2)(n+3)}A_n'''''''(z)r^6 - \ldots \end{aligned} \tag{5}$$

In analogy to Equations 4 and 5 we write :

$$g_{zn}(r,z) = \sum_{k=0} (-1)^{k+1} \frac{n!}{2^{2k} k!(n+k)!} A_n^{(2k+1)} r^{2k} \tag{6}$$

or explicitly :

$$g_{zn}(r,z) = -A_n^{'}(z) + \frac{1}{4(n+1)} A_n^{'''}(z) r^2 - \frac{1}{32(n+1)(n+2)} A_n^{'''''}(z) r^4 ..... \tag{7}$$

We have computed g_m , $g_{\theta n}$ and g_{zn} from which the A(z) and its derivatives have been computed. In the following figures we show results for the A's derived from the conductor only, the iron only, and both iron and conductor together. For the conductor alone the A's have been computed up to $\frac{\partial^4 A(z)}{\partial z^4}$ for n=2,6,10,14 and 18. The quality of the iron contribution at the present time is limited and therefor the A's for the iron have been computed only to $\frac{\partial^2 A(z)}{\partial z^2}$ for n=2,6 and 10. For the conductor+iron case we have carried the A's up to n=14.

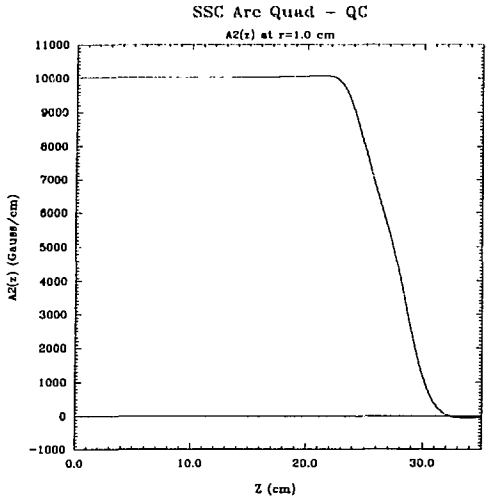

Figure 16 The quad function (n=2) A2(z) — CONDUCTOR ONLY.

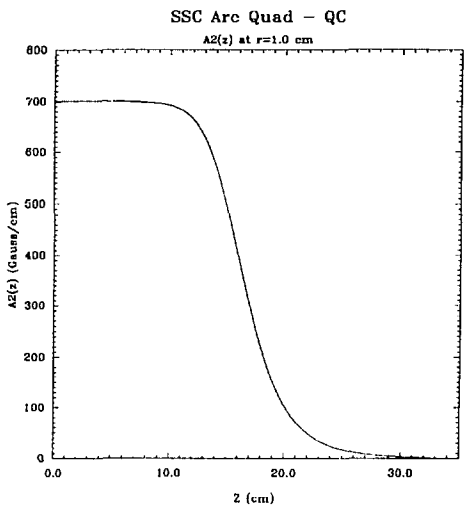

Figure 17 The quad function (n=2) A2(z) — IRON ONLY.

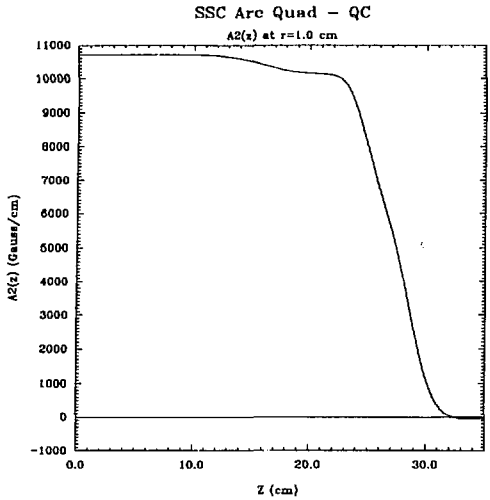

Figure 18 The quad function (n=2) A2(z) — CONDUCTOR and IRON.

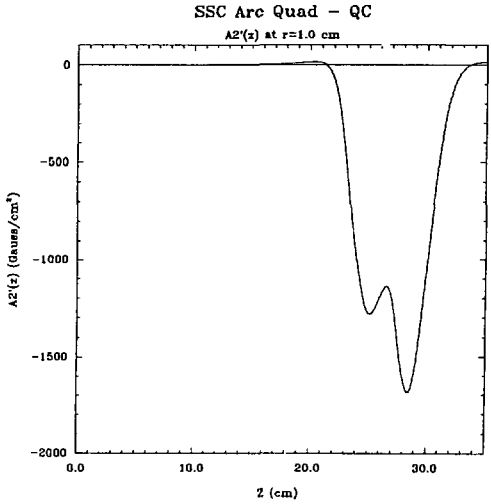

Figure 19 The first derivative function of n=2 — A2'(z) — CONDUCTOR ONLY.

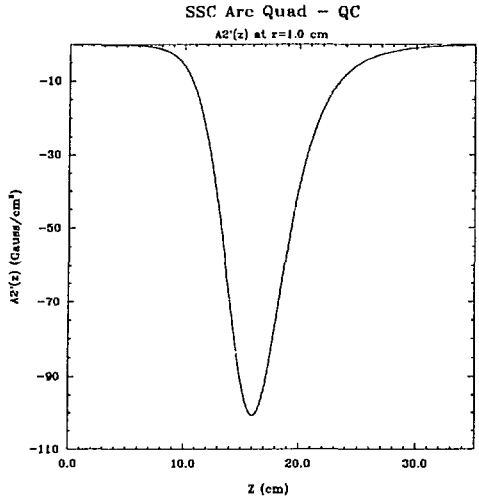

Figure 20 The first derivative function of n=2 — A2'(z) — IRON ONLY .

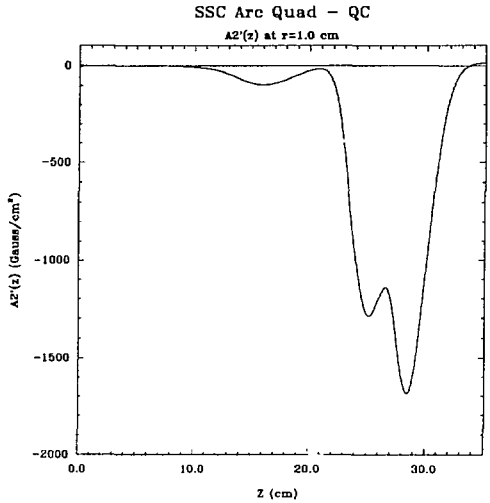

Figure 21 The first derivative function of n=2 — A2'(z) — CONDUCTOR and IRON.

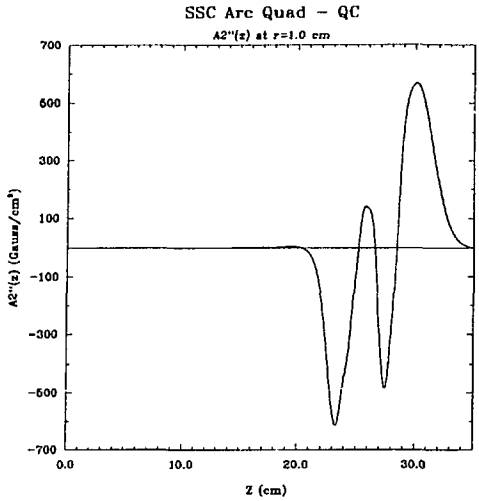

Figure 22 The second derivative function of n=2 — A2"(z) — CONDUCTOR ONLY.

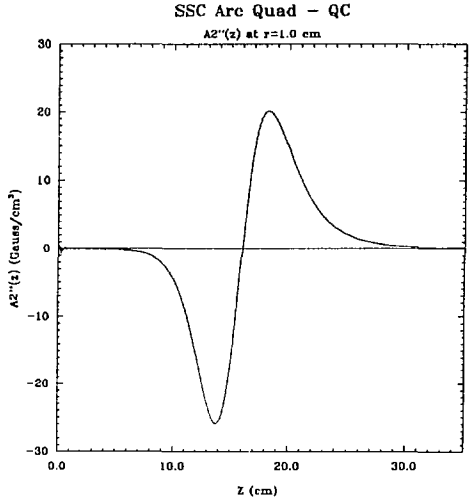

Figure 23 The second derivative function of n=2 — A2"(z) — IRON ONLY.

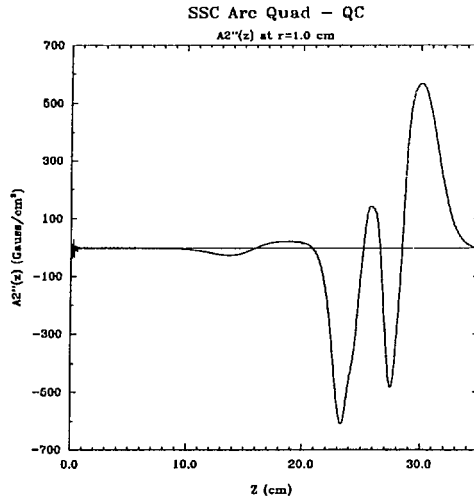

Figure 24 The second derivative function of n=2 — A2''(z) — CONDUCTOR and IRON.

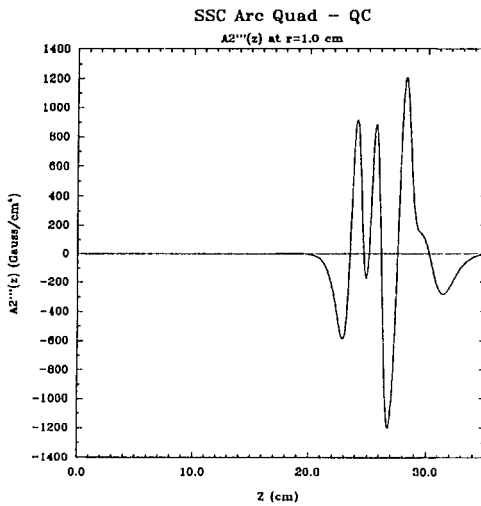

Figure 25 The 3-rd derivative function of n=2 — A2'''(z) — CONDUCTOR ONLY.

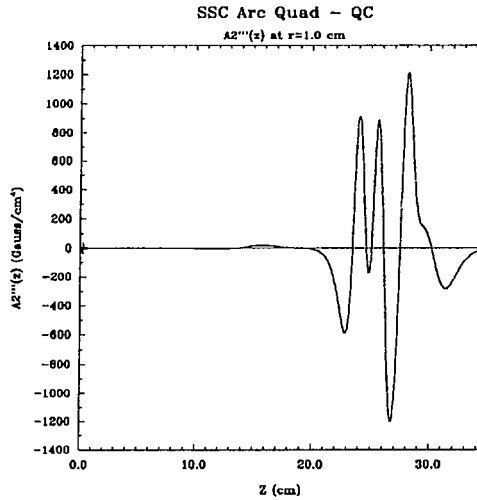

Figure 26 The 3-rd derivative function of n=2 — A2'''(z) — CONDUCTOR and IRON.

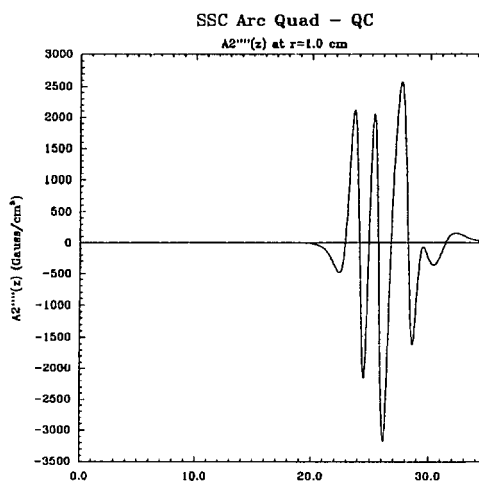

Figure 27 The fourth derivative function of n=2 — A2''''(z) — CONDUCTOR ONLY.

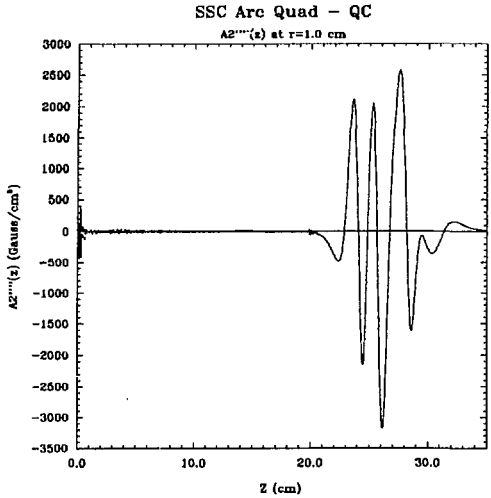

Figure 28 The fourth derivative function of n=2 — A2''''(z) — CONDUCTOR and IRON.

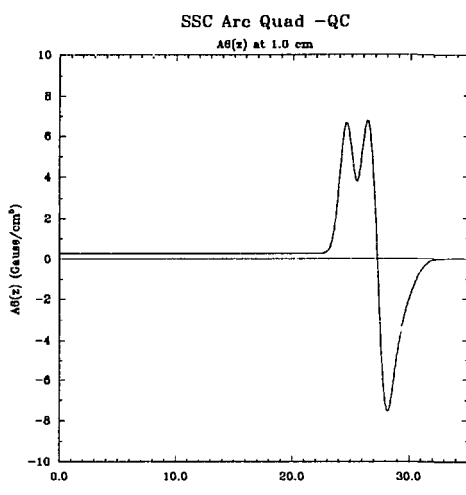

Figure 29 The dodecapole function A6(z) — CONDUCTOR ONLY.

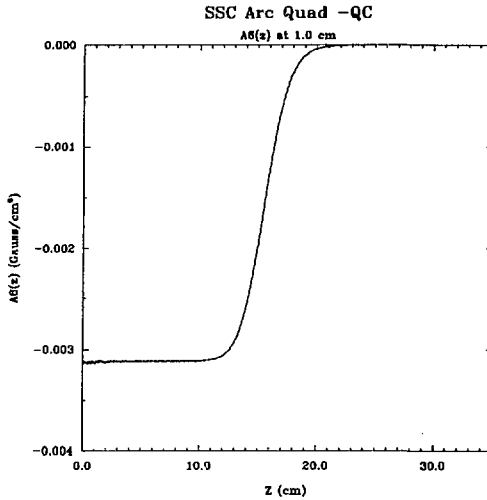

Figure 30 The dodecapole function A6(z) — IRON ONLY.

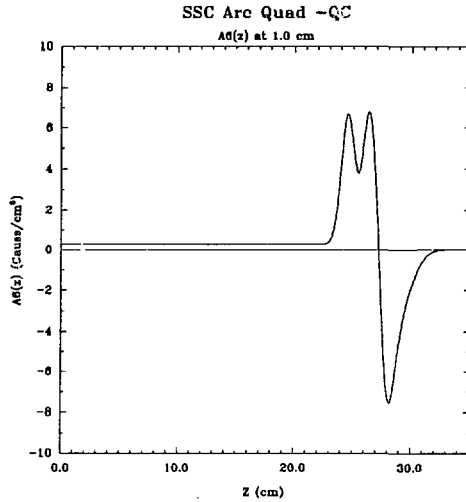

Figure 31 The dodecapole function A6(z) — CONDUCTOR and IRON.

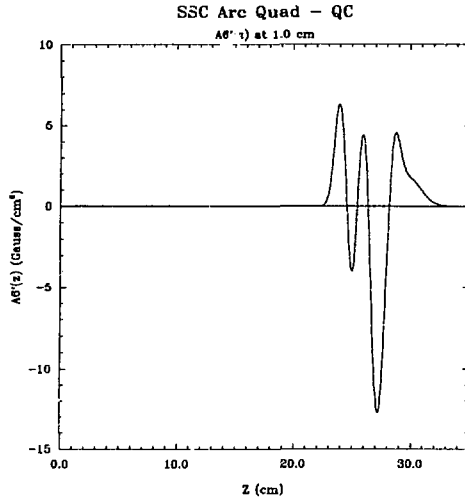

Figure 32 The first derivative function of n=6 — A6'(z) — CONDUCTOR ONLY.

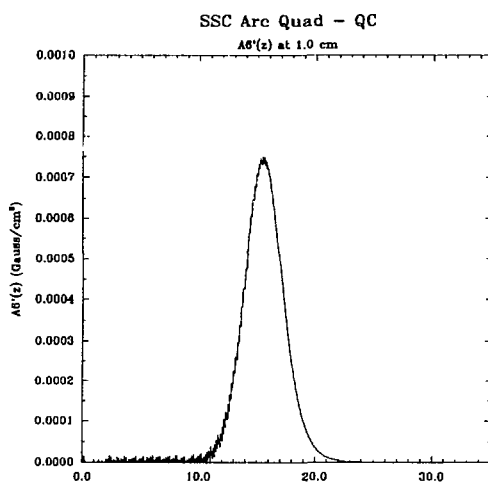

Figure 33 The first derivative function of n=6 — A6'(z) — IRON ONLY.

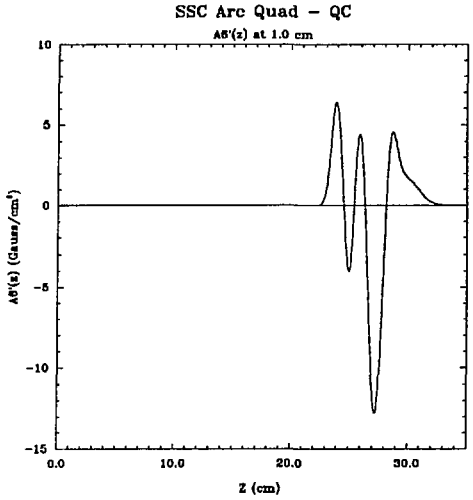

Figure 34 The first derivative function of n=6 — A6'(z) — CONDUCTOR and IRON.

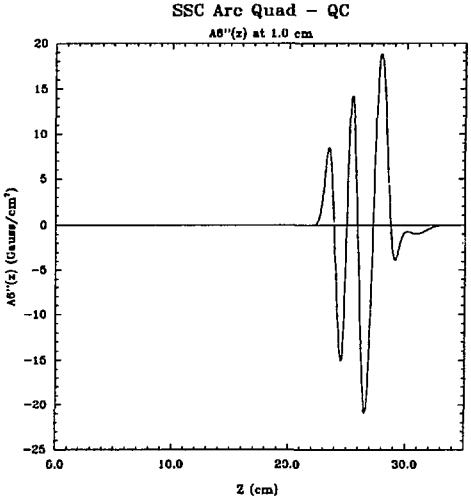

Figure 35 The second derivative function of n=6 — A6''(z) — CONDUCTOR ONLY.

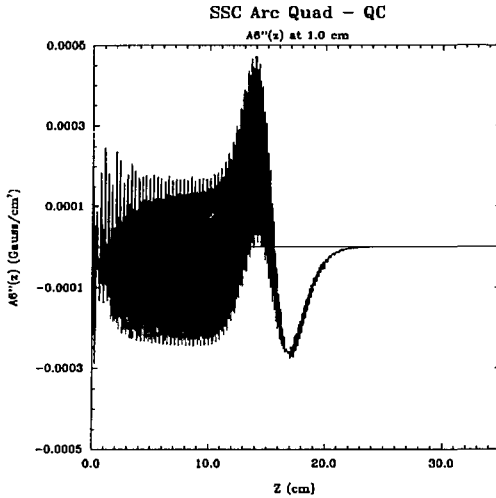

Figure 36 The second derivative function of n=6 — A6"(z) — IRON ONLY.

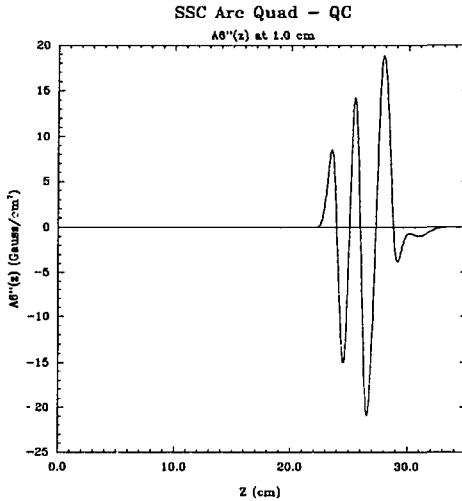

Figure 37 The second derivative function of n=6 — A6"(z) — CONDUCTOR and IRON.

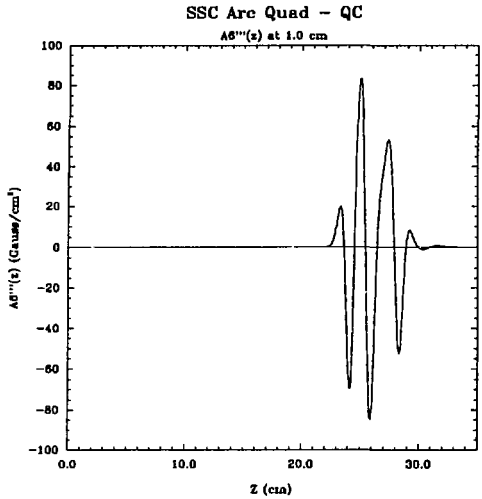

Figure 38 The 3-rd derivative function of n=6 — A6'''(z) — CONDUCTOR ONLY.

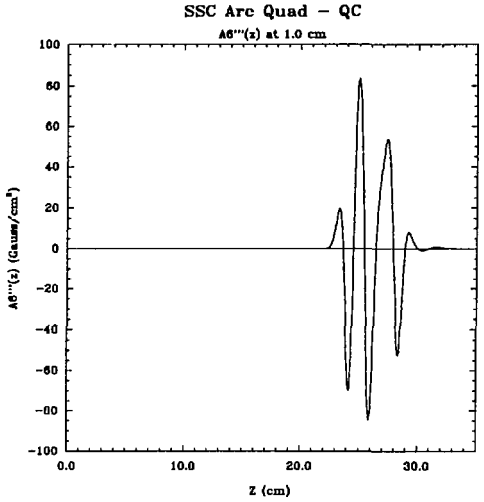

Figure 39 The 3-rd derivative function of n=6 — A6'''(z) — CONDUCTOR and IRON.

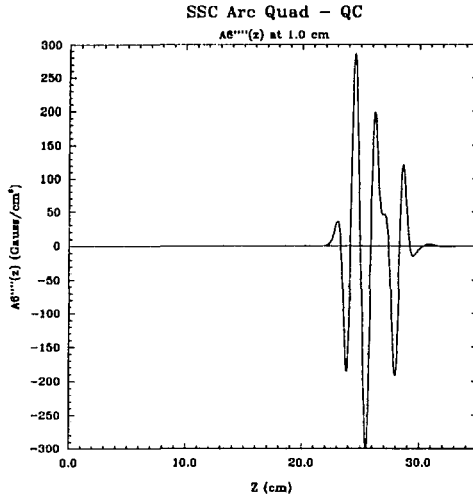

Figure 40 The fourth derivative function of n=6— A6''''(z) — CONDUCTOR ONLY.

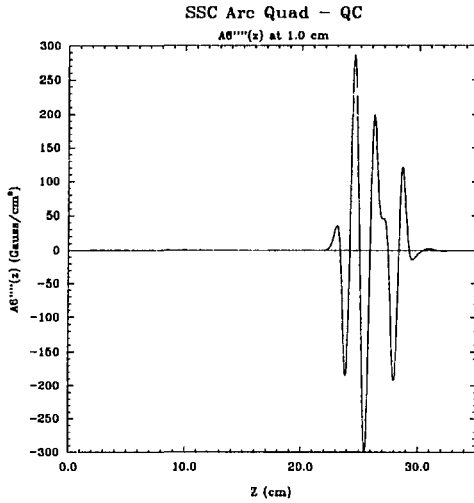

Figure 41 The fourth derivative function of n=6— A6''''(z) — CONDUCTOR and IRON.

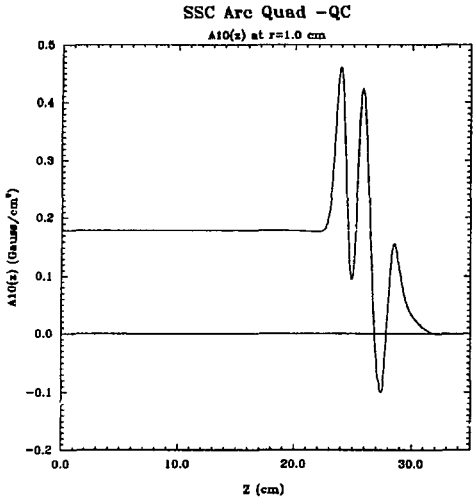

Figure 42 The 20 pole function A10(z) — CONDUCTOR ONLY.

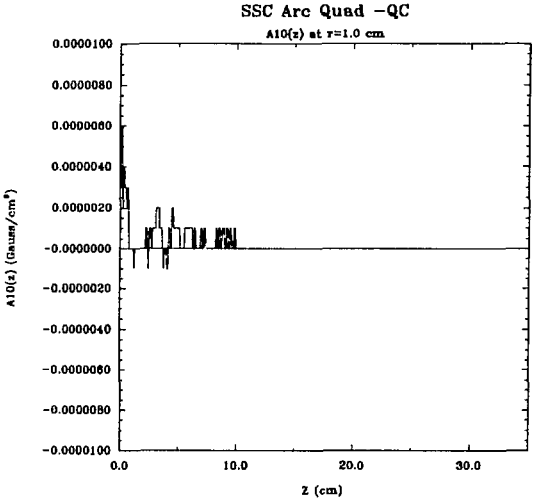

Figure 43 The 20 pole function A10(z) — IRON ONLY.

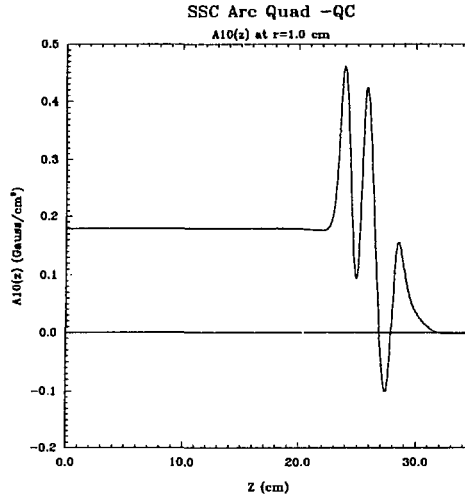

Figure 44 The 20 pole function A10(z) — CONDUCTOR and IRON.

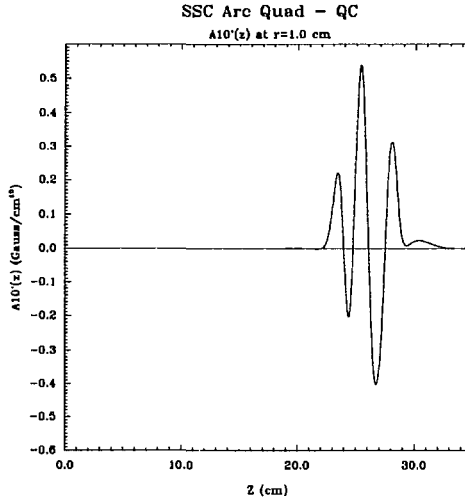

Figure 45 The first derivative function of n=10 — A10'(z) — CONDUCTOR ONLY.

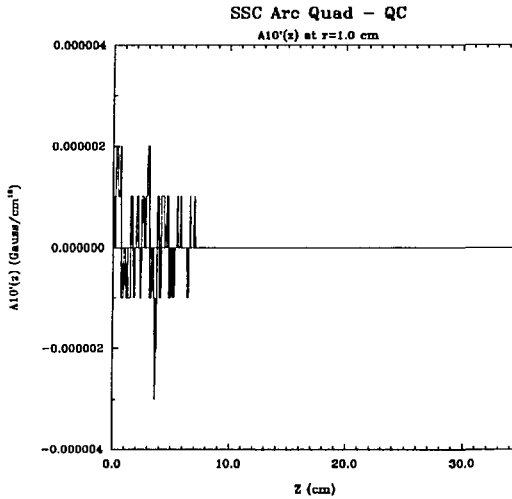

Figure 46 The first derivative function of n=10 — A10'(z) — IRON ONLY.

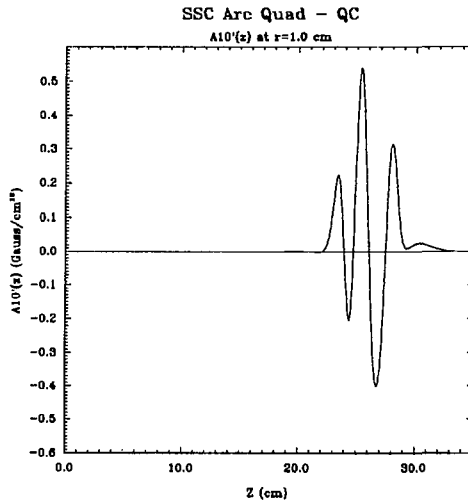

Figure 47 The first derivative function of n=10 — A10'(z) — CONDUCTOR and IRON.

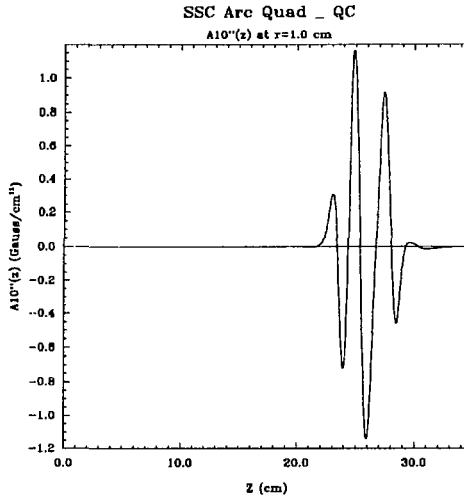

Figure 48 The second derivative function of n=10 — A10"(z) — CONDUCTOR ONLY.

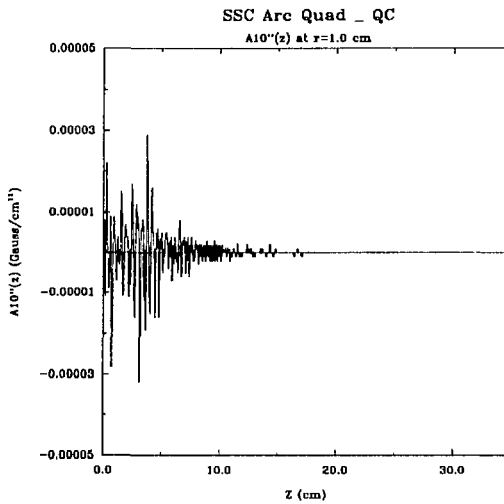

Figure 49 The second derivative function of n=10 — A10"(z) — IRON ONLY.

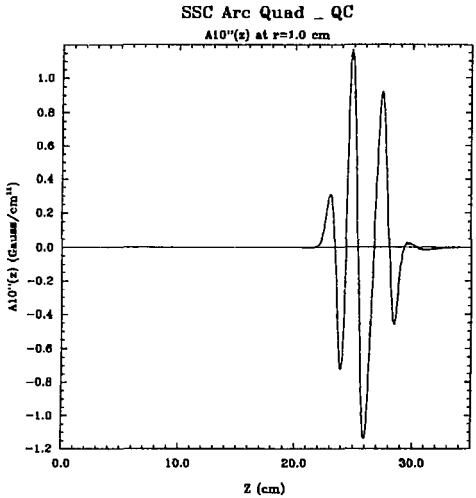

Figure 50 The second derivative function of n=10 — A10''(z) — CONDUCTOR and IRON.

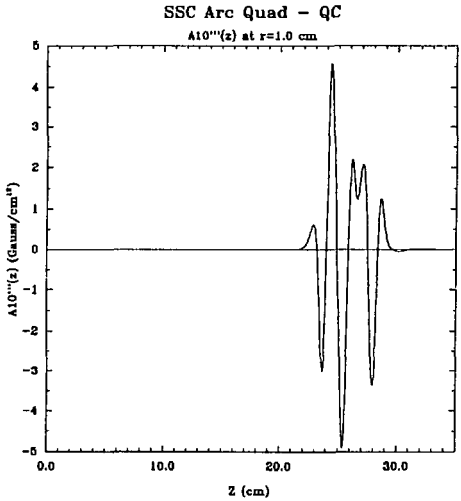

Figure 51 The 3-rd derivative function of n=10 — A10'''(z) — CONDUCTOR ONLY.

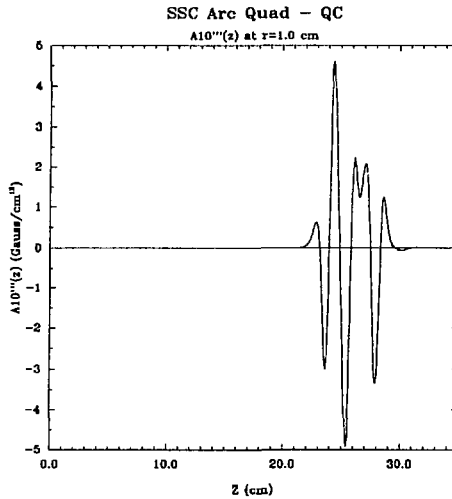

Figure 52 The 3-rd derivative function of n=10 — A10'''(z) — CONDUCTOR and IRON.

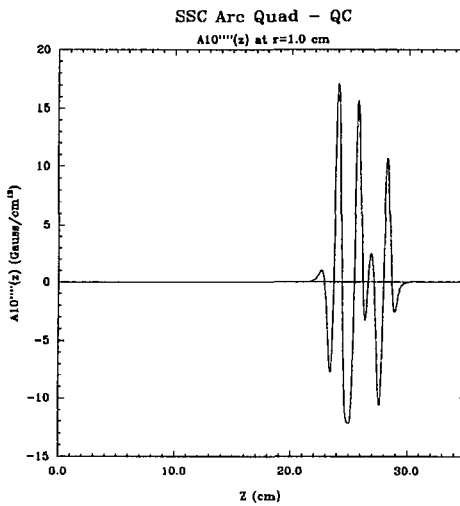

Figure 53 The fourth derivative function of n=10 — A10''''(z) — CONDUCTOR ONLY.

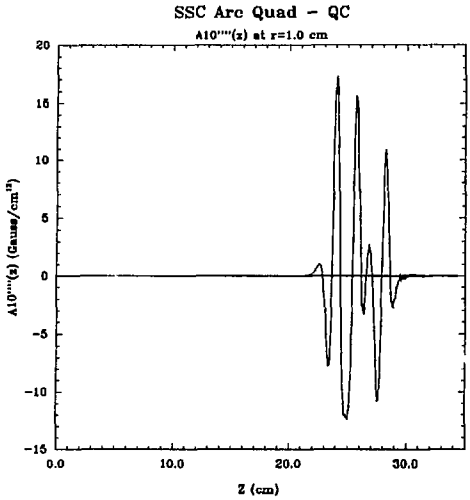

Figure 54 The fourth derivative function of n=10 — A10''''(z) — CONDUCTOR and IRON.

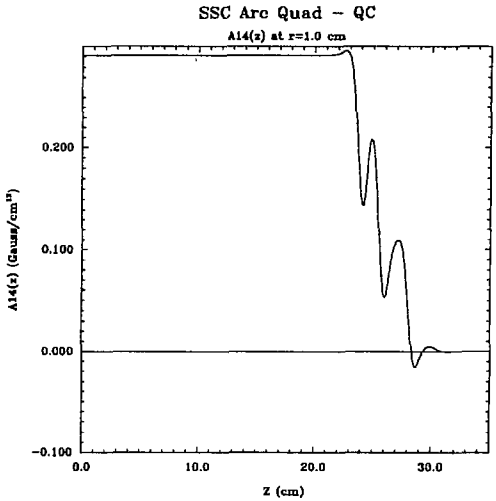

Figure 55 The 28 pole function A14(z) — CONDUCTOR ONLY.

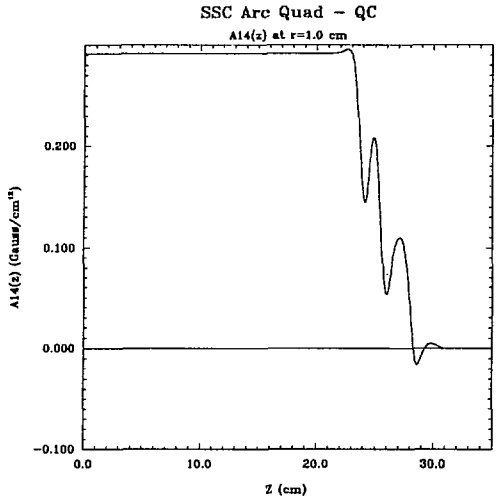

Figure 56 The 28 pole function A14(z) — CONDUCTOR and IRON.

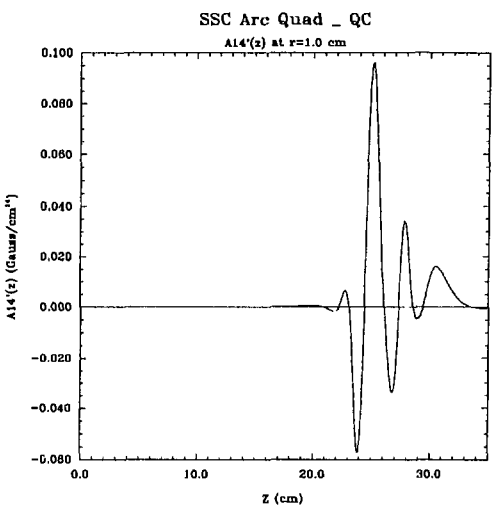

Figure 57 The first derivative function of n=14 — A14'(z) — CONDUCTOR ONLY.

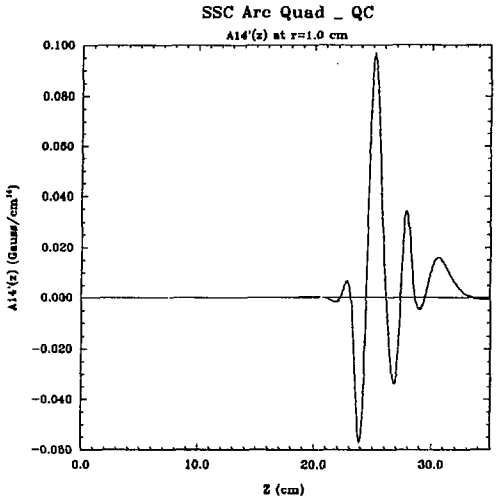

Figure 58 The first derivative function of n=14 — A14'(z) — CONDUCTOR and IRON.

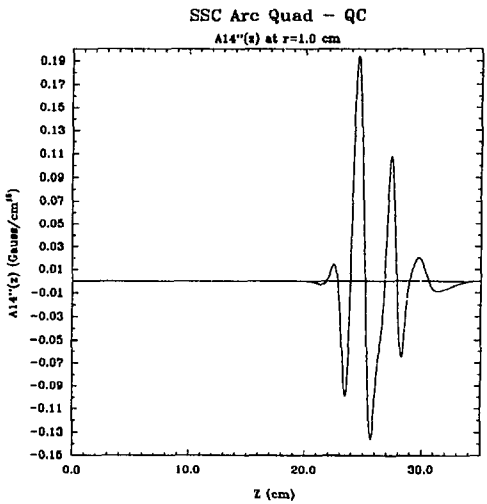

Figure 59 The second derivative function of n=14 — A14"(z) — CONDUCTOR ONLY.

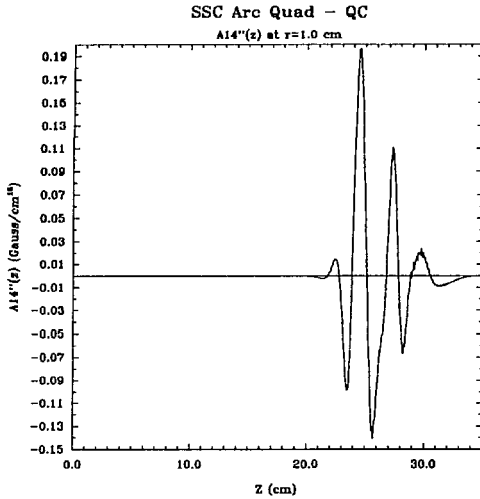

Figure 60 The second derivative function of n=14 — A14"(z) — CONDUCTOR and IRON.

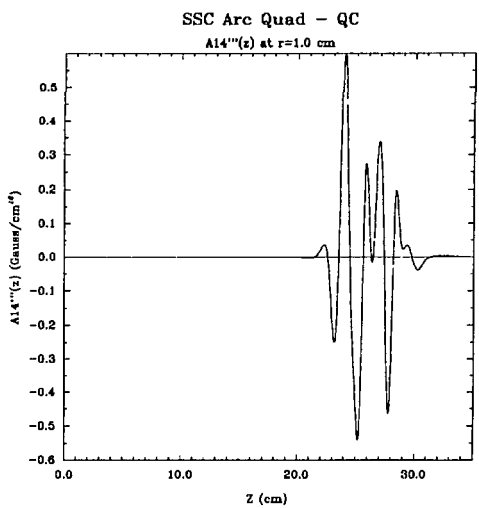

Figure 61 The 3-rd derivative function of n=14 — A14'''(z) — CONDUCTOR ONLY.

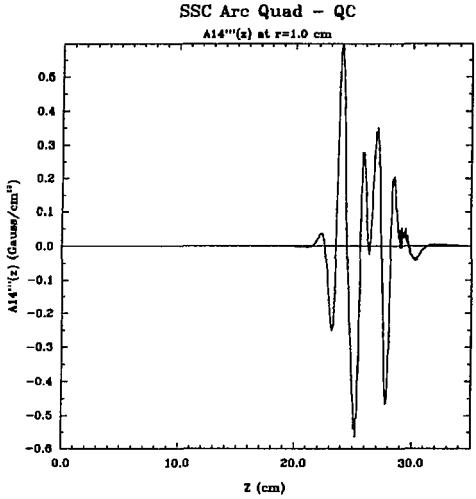

Figure 62 The 3-rd derivative function of n=14 — A14'''(z) — CONDUCTOR and IRON.

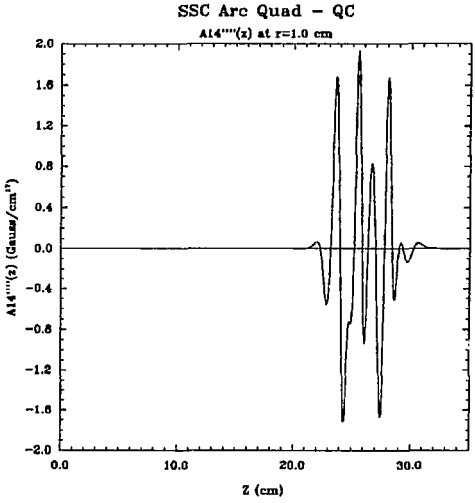

Figure 63 The fourth derivative function of n=14 — A14''''(z) — CONDUCTOR ONLY.

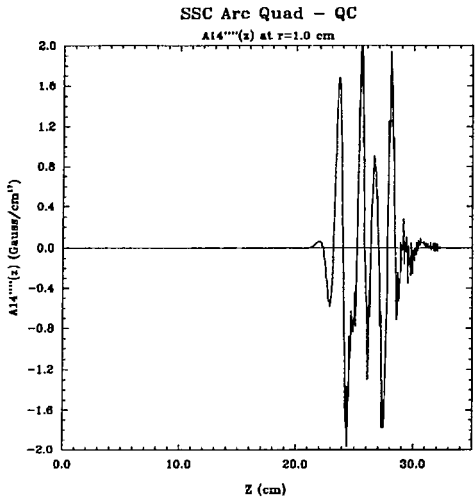

Figure 64 The fourth derivative function of n=14 — A14''''(z) — CONDUCTOR and IRON.

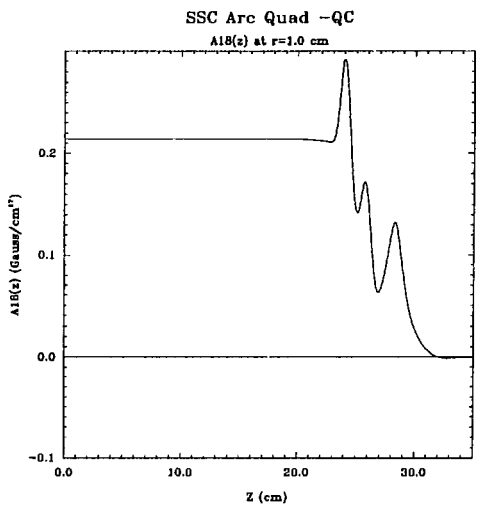

Figure 65 The 36 pole function A18(z) — CONDUCTOR ONLY.

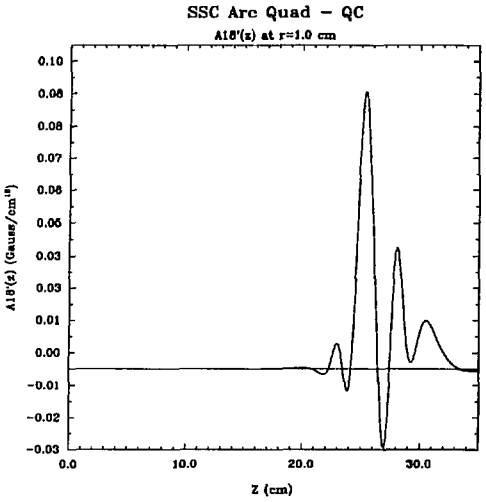

Figure 66 The first derivative function of n=18 — A18'(z) — CONDUCTOR ONLY.

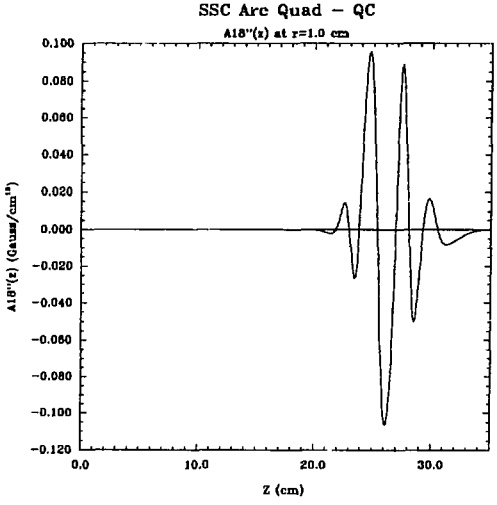

Figure 67 The second derivative function of n=18 — A18''(z) — CONDUCTOR ONLY.

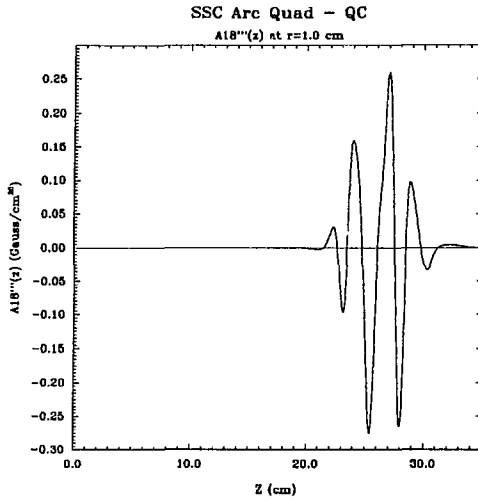

Figure 68 The 3-rd derivative function of n=18 — A18'''(z) — CONDUCTOR ONLY.

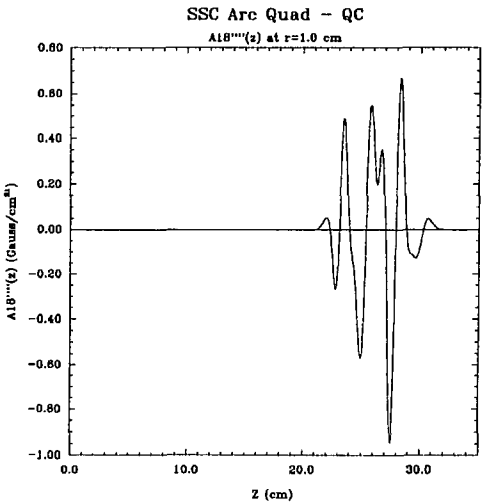

Figure 69 The fourth derivative function of n=18 — A18''''(z) — CONDUCTOR ONLY.